

Isothermal and Cyclic Oxidation Behavior of AISI 430 Ferritic Stainless Steel Coated with Titanium

Saeed Keshavarz¹, Morteza Zandrahimi¹, Hadi Ebrahimifar^{2,*}

¹ Department of Metallurgy and Materials Science, Faculty of Engineering, Shahid Bahonar University of Kerman, Jomhoori Eslami Blvd., Kerman, Iran.

² Department of Materials Engineering, Faculty of Mechanical and Materials Engineering, Graduate University of Advanced Technology, 7631133131, Kerman, Iran.

ARTICLE INFO

Article history:

Received 27 August 2017

Accepted 14 June 2018

Available online 15 September 2018

Keywords:

AISI 430 stainless steel

Titanium

Pack cementation

Oxidation

ABSTRACT

In order to improve the oxidation resistance of ferritic stainless steel, it is possible to deposit a protective coating onto the steel substrate. In this research, through the usage of pack cementation method a coating of titanium was applied on the surface of AISI 430 stainless steel. Scanning Electron-Microscopy (SEM), Energy-Dispersive X-ray spectrometry (EDAX) and X-ray diffraction (XRD) were used for evaluating of coating structure. Results showed that titanium coating consisted of two layers with the total thickness of 50 micron. The titanized layer consisted of TiFe, TiFe₂ and Fe₂TiO₅ phases. For investigating the oxidation behavior of the coated and uncoated specimens, isothermal and cyclic oxidation tests were performed at 1000 °C. In isothermal oxidation, the oxidation resistance of the titanium coated specimens was improved by restricting the outward penetration of chromium cation. The results of cyclic oxidation of titanium coated samples indicated that they were resistant to lamination and cracking.

1-Introduction

Development of new materials and coatings for high temperature applications is an important research area. The continuing demand to increase the temperature in combustion chambers and gas turbines in order to enhance the efficiency of the plants will benefit from such researches [1]. Stainless steels have been used in gas turbine engines applications with protective coating to combat oxidation problems in aero engines and hot corrosion in industrial and marine engines [2,3]. The presence of a surface protective coating is generally required to extend the life of the component in high temperature working environments [4, 5]. Protective coatings are predominantly of the

diffusion type and are produced by a variety of techniques such as chemical vapor deposition, pack cementation, slurry coating and hot dipping. For hot section applications, diffusion coatings that are reproduced by pack cementation process and are still predominant in the gas turbine industry and currently serve 80 to 90 percent of the world market [5].

Pack cementation processes are categorized as low activity and high activity packs based on the amount of activator. In low activity packs (a low amount of activators) the coating is produced by outward diffusion of the substrate atoms while in the high activity packs (high amount of activator), the coating is produced by inward diffusion of the coating elements. In the case of

* Corresponding author:

E-mail address: H.Ebrahimifar@kgut.ac.ir

external growth, any particles from the pack will be easily entrapped in the coating [6, 7].

Pack cementation is a comparatively easy technique, which includes immersing the component to be coated in a powder mixture in a sealed or semi-sealed retort [8, 9]. The pack cementation process is simple to reproduce. In the pack process, the driving force for the transfer of coating element is the difference in activity between the source and the substrate surface [10].

Pack-titanizing has been extensively employed for steels and super alloys to improve their hot temperature oxidation resistance [11]. The coating can form titanium oxides or intermetallic compounds, which are highly resistant to oxidation and hot corrosion at elevated temperature and hostile environment [11].

The intermetallic compounds (especially titanium intermetallics) are interesting structural materials for high temperature applications due to their favorable properties, for instance low specific weight, high strength and good corrosion resistance at elevated temperatures, and reasonably good ductility at ambient temperature [12-15].

Up to now no research has been done about the influence of diffusional coating of titanium on the oxidation resistance of AISI 430 at high temperatures. The aim of this research was to deposit titanium coating onto AISI 430 stainless steel. Isothermal oxidation for studying grown oxides at 1000 °C and cyclic oxidation for applying thermal stresses on the uncoated and coated specimens were carried out. Also, surface scale structures of coated and uncoated AISI 430 steel after isothermal and cyclic oxidation were investigated.

2- Materials and methods

2-1- Materials

AISI 430 stainless steel was used as the substrate. The chemical composition of the substrate is shown in Table 1. The coupons were ground up to 1200 grit SiC paper, cleaned and ultrasonically degreased in acetone and methanol.

For pack titanizing process, pure titanium powder was used as the metal source, ammonium chlorine powder as the activator and alumina as the inert filler. The average particle

size of titanium was 1 µm and that of ammonium chloride and alumina was 5 µm.

Table 1. Chemical composition of AISI 430 stainless steel

Element	C	Cr	Mn	Si	S	P	Fe
Concentration (wt. %)	0.12	17.5	0.85	0.75	0.02	0.03	Balance

2-2- Coating process

AISI 430 samples were enclosed in a stainless steel box filled with the powder mixture and sealed. In order to deposit titanium onto the AISI 430 substrate, pack cementation method was employed. Ti, Al₂O₃ and NH₄Cl powder were used as powder mixture with the average size of 20 µm, 40 µm and 180 µm, respectively. The optimized conditions for coating of titanium onto the AISI 430 stainless steel were identified: 15% w.t. Ti, 5% w.t. NH₄Cl, 85% w.t. Al₂O₃ as powder mixture and heating at 950 °C for 6 h in argon gas atmosphere.

After the coating process, the samples were cooled down to room temperature in the circulation of inert gas. A steady flow of argon (0.35 lit/min) was maintained during both the coating process and the cooling cycle. The optimum time was determined according to the layer thickness and the final coating structure.

After pack cementation treatment, the samples were removed from the pack and ultrasonically cleaned in ethanol to remove any embedded pack material and then weighed using an electronic balance.

2-3- Evaluation techniques

After pack cementation, the coated specimens were lightly polished to remove any particles sticking to the specimen surface from the powder pack. The cross section of Ti-coated samples was examined by using optical microscopy and scanning electron microscopy (SEM) equipped with EDS analyzer. Diffusion profiles of Ti across the coating were derived by EDS. X-Ray diffraction (XRD) with Cu-Kα radiation operating at 40kV and 30mA (Phillips X'Pert) was used to identify the phases formed in the coatings. To investigate the oxidation behavior of the as-coated samples, isothermal and cyclic oxidations were carried out at 1000

°C in air in an electrical furnace. The samples were weighted at room temperature for several times by electronic balance with a sensitivity of 0.1 mg during oxidation at 1000 °C.

3- Results and discussion

3-1- Titanizing

Fig. 1 demonstrates the cross-section SEM image (Fig. 1a) and the concentration profiles of titanium and the major elements (Fig. 1b) in the coating layer measured by EDS. The element

concentration profiles confirm the deposition of titanium from the vapour phase, which resulted in the formation of a uniform coating layer rich in titanium. As can be seen, the total thickness of the coating is about 50µm. The coating consists of two different layers; the outer layer is 40 µm thick and the inner layer is 10µm thick. As can be seen, the concentration of Ti at the surface is about 42.%. In the outer layer the concentration of Ti is about 64 % which increases to 75 % in the inner layer and decreases to 3 % in the substrate.

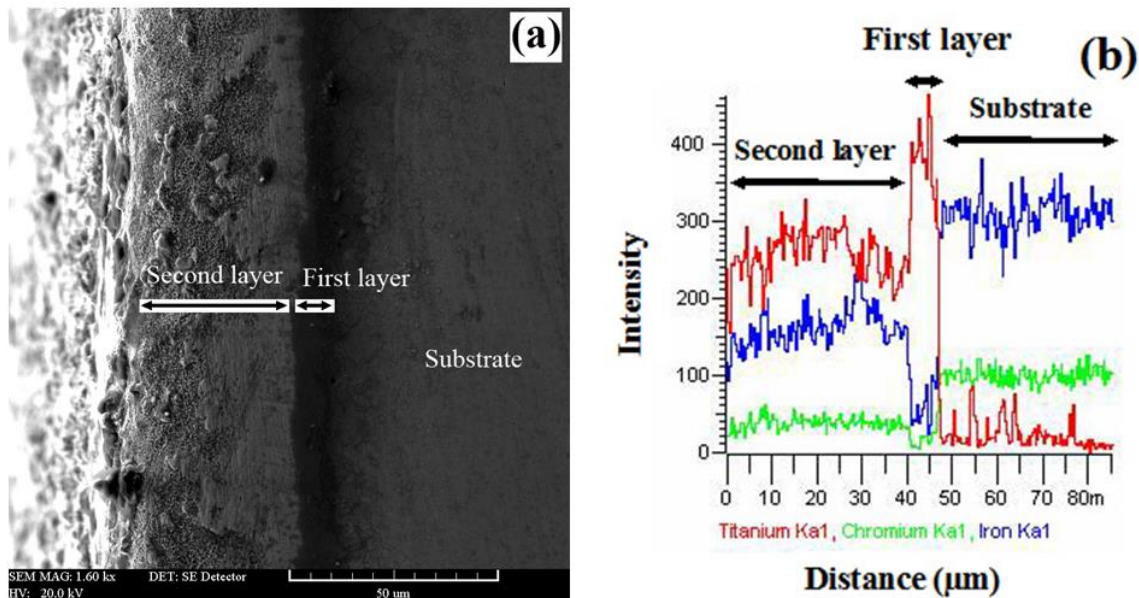


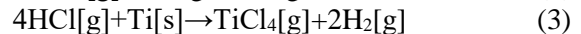
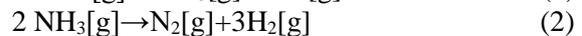
Fig. 1. SEM cross section image (a) and EDS line scan (b) of the coated sample.

Test under the optical microscope demonstrated the presence of pack alumina particles in the top surface of the titanium coating. This is a typical feature, suggesting that the coating was created via an outward growth process involving Ti enrichment and the outward migration of substrate elements, Cr and Fe in particular [16]. Another reason is the temperature of coating and the amount of activator [11, 12]. If pack cementation process is conducted at high temperature and in low activity pack, an external Ti-Fe layer is formed on the surface by dominant outward diffusion of Fe (Figure 1).

X-ray diffraction pattern from the coated sample shows the presence of TiFe, TiFe₂ and Fe₂TiO₅ phases (Fig. 2). The presence of TiFe and TiFe₂ in the X-ray diffraction pattern (Fig. 2) is due to inter diffusion between titanium and iron at

elevated temperatures and in the intermediate coating layer.

During the experiment, the active Ti was probably created by the following reactions:



and therefore the formation of TiFe and TiFe₂ based on the active Ti is carried out through the following reactions:



TiFe and TiFe₂ are intermetallic compounds which have good oxidation resistance [11]. They improve the high-temperature performance of coated AISI 430. Fe₂TiO₅ phase is formed as a result of oxidation of TiFe and TiFe₂ with

entrapped oxygen in the pack. The interruption of oxygen in the pack mixture is a common matter which was observed in the previous researches [16].

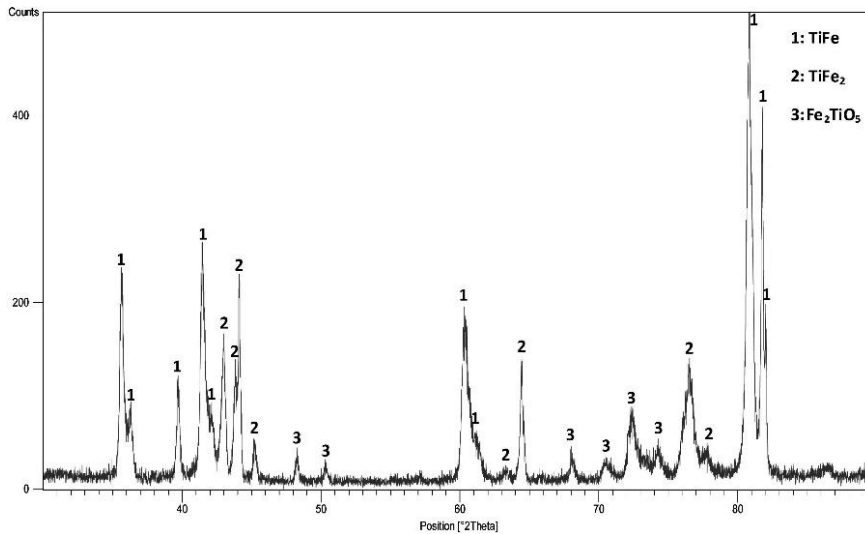


Fig. 2. XRD pattern of coated specimen.

3-2- Isothermal oxidation behavior

Isothermal oxidation of Ti-coated and uncoated AISI 430 samples was studied in static air at 1000 °C for 200 h. Fig. 3 shows the mass gain for Ti-coated and uncoated AISI 430 specimens as a function of the oxidation time at 1000 °C. As can be seen, the mass gain increases with the oxidation time during the initial oxidation stage for uncoated steel (0-20 hours) and for Ti-coated steel (0-20 hours). After that, the mass gain increases slightly with the oxidation time during the second stage. For

the uncoated AISI 430 steel, by increasing the oxidation time, the weight gain enhances slightly. It is due to the creation of a protective layer which is consistent with previous works [16, 17].

For the uncoated samples, the rate of initial oxidation is higher than the Ti-coated samples. It is because of the non-protective surface of the uncoated steel which results in the higher growth rate of oxide scales [18]. The concentration of Cr at the oxide/metal interface by growth of Cr-containing oxides increases in the initial period of oxidation.

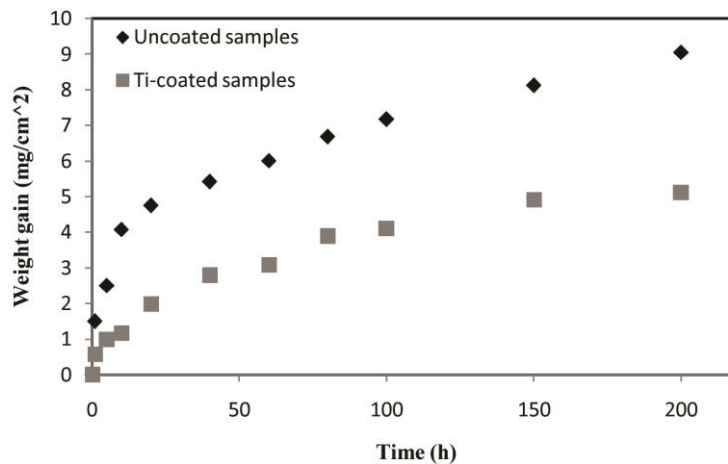


Fig. 3. Mass gain as a function of oxidation time in isothermal oxidation for the uncoated and coated samples.

At the second stage for more growth, Cr should be provided by diffusion from the 304 steel. The diffusion of Cr in the 430 steel may be rate limiting for oxidation until the oxide scale growth slows down due to its parabolic kinetics [18-21]. For the coated steels, titanium diffusional coating became stabilized in the second stage and demonstrated a lower oxidation rate in comparison with the first stage.

For both specimens the behavior of isothermal oxidation follows the parabolic rate law, indicating that the oxide scales which are formed on the surfaces can act as a diffusion barrier [17].

As can be seen, all the Ti-coated samples show smaller mass gain in comparison with the bare substrates at various oxidation times. The rate of oxidation is decreased by titanium coating layer, which is consistent with the expectation based on the oxide scale characterization. The bare substrate after 200 h of isothermal oxidation had a weight change of 9.05 mgcm⁻², while the Ti-coated samples had a weight change of 5.12 mgcm⁻². It is clearly demonstrated that the coating protects the AISI 430 steel substrate from oxidation at high temperatures.

Fig. 4 shows the square of mass gain versus the time of oxidation for the uncoated and Ti-coated AISI 430 stainless steel at 1000 °C.

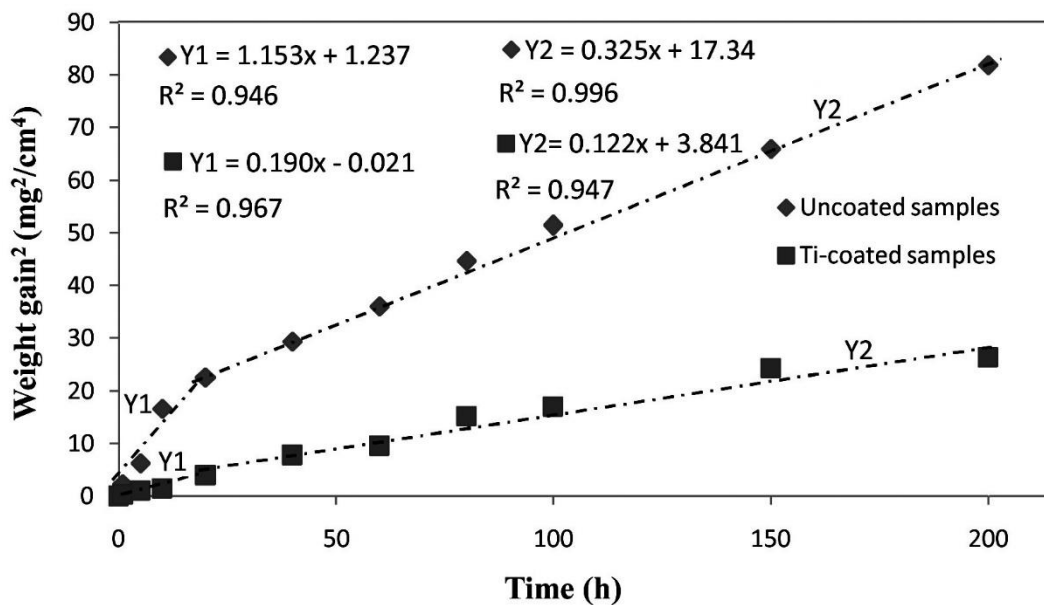


Fig. 4. Square of mass gain as a function of oxidation time in isothermal oxidation for coated and uncoated samples.

As illustrated, the mass gain of uncoated samples enhances parabolically with the increase of isothermal oxidation time which satisfies the parabolic kinetics law explained by

$$\left(\frac{\Delta W}{A}\right)^2 = k_p t \tag{1}$$

where ΔW is the mass gain, A is the surface area of the sample, k_p is the parabolic rate constant, and t is the time of oxidation. The parabolic behavior of the uncoated and Ti-coated AISI 430 steel is due to the growth of

chromia (Cr₂O₃) scale which followed the parabolic rate law [22].

The growth of oxide scales is because of the inward diffusion of oxygen and outward diffusion of manganese, iron, and chromium. Since the oxidized coating gets thicker, the growth rate gets slower due to longer distances of diffusion. Therefore, the oxidation kinetics of titanium coating layer could be estimated by the average thickness of oxide scales, which was explained by the parabolic law.

Two stages of oxidation can be seen in both groups of samples. According to the parabolic

law [23], the value of k_p for uncoated steel at the first (between 0 and 20 h) and second (between 20 and 200 h) stages is $2.125 \times 10^{-11} \text{ g}^2\text{cm}^{-4}\text{s}^{-1}$ and $5.015 \times 10^{-13} \text{ g}^2\text{cm}^{-4}\text{s}^{-1}$, respectively. For Ti-coated samples the value of k_p in the range of 0-20 h was calculated about $2.638 \times 10^{-12} \text{ g}^2\text{cm}^{-4}\text{s}^{-1}$. According to the oxidation kinetics, it is indicated that a protective oxide scale should be thermally formed between the substrate and the oxidized coating which is created during the first oxidation stage [24, 25]. The square of mass gain as a function of oxidation time for the titanium coating in the range of 20-200 h was $1.882 \times 10^{-13} \text{ g}^2\text{cm}^{-4}\text{s}^{-1}$. This value is lower than of the initial oxidation. The lower value of k_p for the Ti-coated samples in the

second stage ($1.882 \times 10^{-13} \text{ g}^2\text{cm}^{-4}\text{s}^{-1}$) in comparison with the k_p of uncoated AISI 430 steel in the same stage ($5.015 \times 10^{-13} \text{ g}^2\text{cm}^{-4}\text{s}^{-1}$) implies that the diffusion of ions is limited through the use of diffusional titanium coating layer.

After 200 h of isothermal oxidation, the uncoated sample grew a black oxide scale which spilled from the surface in some areas, while the Ti-coated sample (Fig. 5b) exhibited a grey, shiny surface. Fig. 5 shows SEM micrographs of the uncoated (Fig. 5a) and Ti-coated (Fig. 5b) sample after 200 h isothermal oxidation at 1000 °C. Some hexagonal-shaped particles are observed in the micrograph of the uncoated sample (Fig. 5a), which was also observed by other researchers [26].

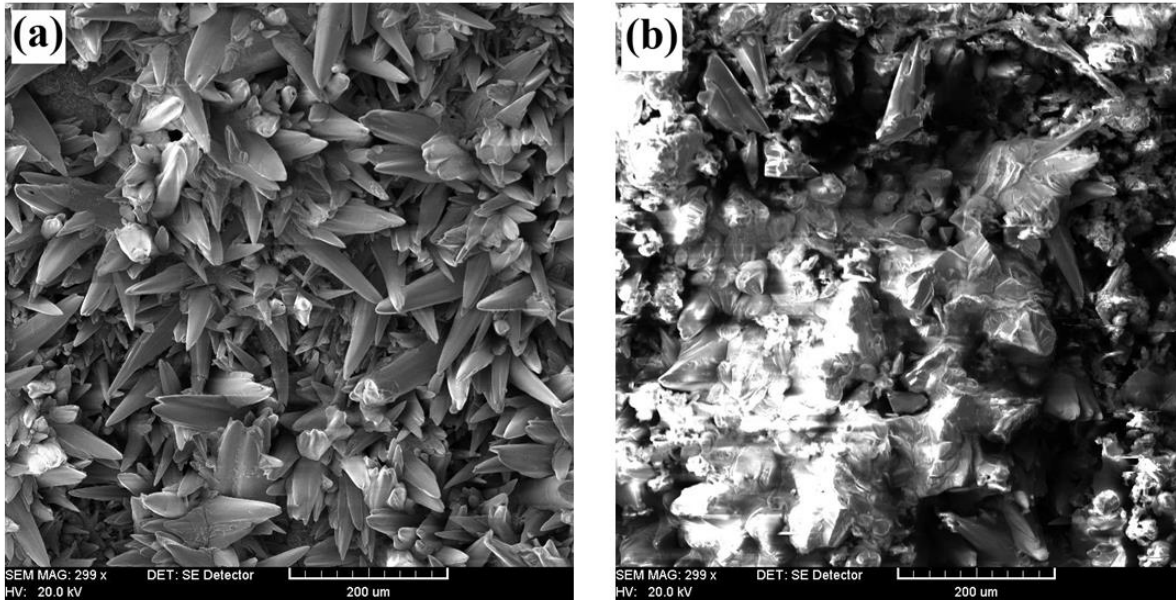


Fig. 5. SEM micrographs of (a) uncoated and (b) coated sample after 200 h isothermal oxidation at 1000°C.

Fig. 6 demonstrates the XRD pattern of the uncoated and Ti-coated samples after 200 h of oxidation. In the XRD pattern of bare substrate (Fig. 6a) $(\text{Mn,Cr})_3\text{O}_4$ spinel, Fe_2O_3 , chromia and silica are observed. The formation of $(\text{Mn,Cr})_3\text{O}_4$ spinel in the uncoated sample is related to ferritic steels that normally contain small amounts of Mn. When steel is subjected to the temperature range of 650 – 850 °C, the spinel layer of $(\text{Mn,Cr})_3\text{O}_4$ will be created [27]. Also, chromia will be formed under the $(\text{Mn,Cr})_3\text{O}_4$ spinel layer [17]. The precipitation of the $(\text{Cr,Mn})_3\text{O}_4$ spinel on the top of the chromia scale can be ascribed to

the high diffusion coefficients of manganese ions. The metal ion diffusion is reduced in the order of $D_{\text{Mn}} > D_{\text{Fe}} > D_{\text{Cr}}$ by supposing that these metal ions diffuse via Cr^{3+} -lattice sites in Cr_2O_3 [28]. Based on the Cr–Mn–O system phase diagram the $(\text{Mn,Cr})_3\text{O}_4$ spinel is thermodynamically favorable even at low Mn concentration [29]. The formation of the $(\text{Mn,Cr})_3\text{O}_4$ spinel layer on the oxide scale could decline significantly the vaporization pressure of gaseous chromium species. Non-protective substrate against oxidation reactions redounded to the creation of these

phases which decrease the electrical conductivity of interconnects [30].

The formation of silica occurs in steels which contain Si in amounts greater than 0.5 wt%.

Insulating, continuous or network-like films of silica can also be grown under the chromia scale [27].

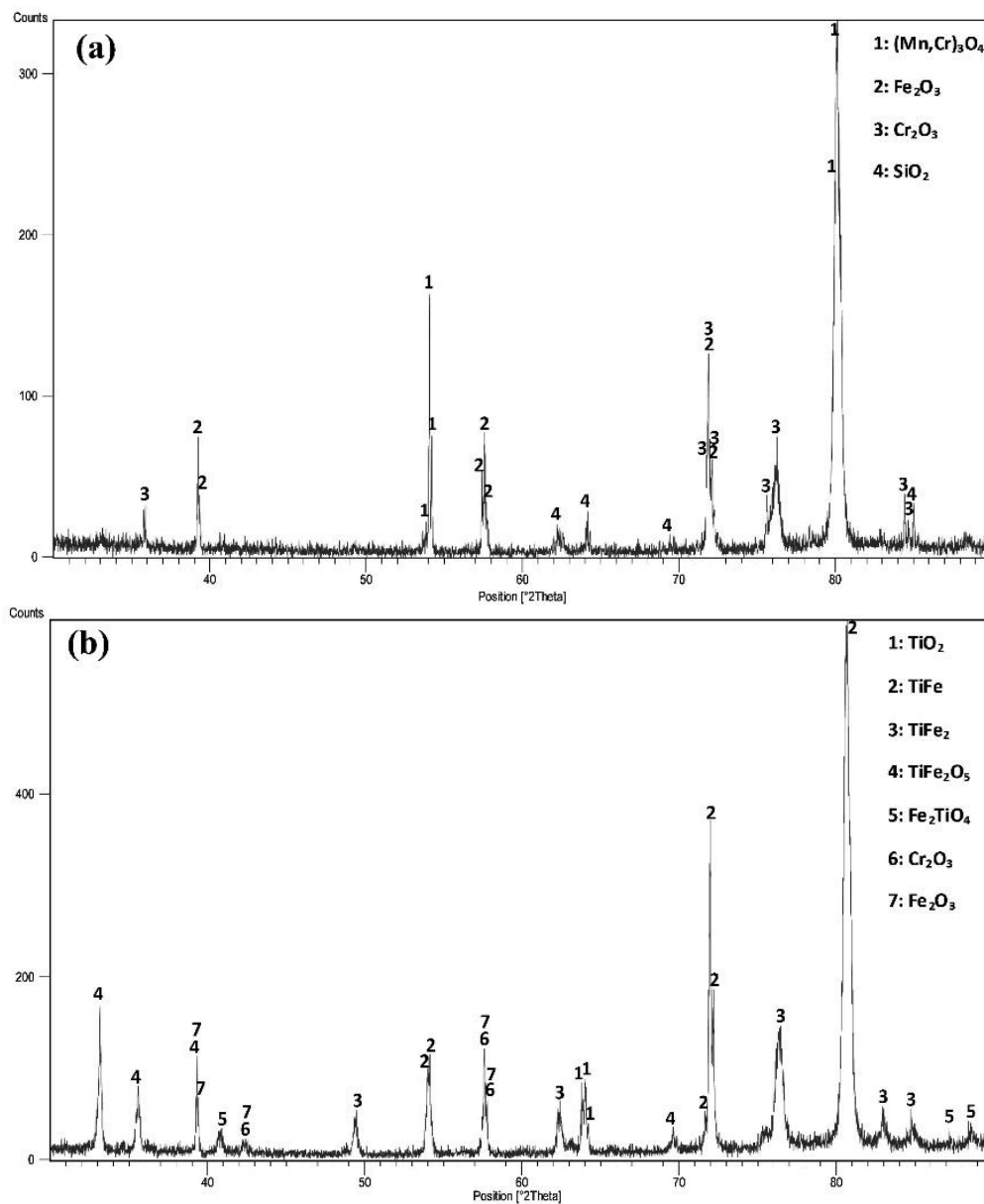


Fig. 6. XRD pattern of (a) uncoated and (b) coated specimens after 200 h isothermal oxidation at 1000 °C.

In the XRD pattern of the coated substrate (Fig. 6b) TiO_2 , TiFe , TiFe_2 , TiFe_2O_5 and Fe_2TiO_4 are observed. The main constituents of titanium-iron will form thermodynamically very stable oxides under oxidizing conditions at high temperatures [15]. The formation of protective titanium oxide scale is essential to provide long-term oxidation resistance at elevated temperatures. On the other hand, titanium oxides

grow very fast and limit the upper temperature capability of titanium alloys to approximately 550 °C. According to thermodynamic calculations, titanium-iron compounds with more than 48-50 titanium atomic percent are expected to form slowly growing titanium oxide scales [31].

The formation of titanium oxides (TiO_2 , TiFe_2O_5 and Fe_2TiO_4) and also the existence of titanium

intermetallics (TiFe , TiFe_2) during the isothermal oxidation improved the oxidation resistance. Weight change results (Fig. 3) indicate that the diffusional titanium coating layer performs as an effective obstacle against outward diffusion of Cr cation and inward diffusion of oxygen anion [31, 32]. Fe_2O_3 and Cr_2O_3 are also observed in the XRD pattern of oxidized Ti-coated sample, but the lower intensity of these phases indicates that the

formation of these peaks has been restricted. Titanium diffusional coating limited the interaction of chromium, iron and oxygen, so the formation of chromia and hematite has been restricted [32].

Fig. 7 demonstrates the SEM cross-sectional image of uncoated (Fig. 7a) and Ti-coated sample (Figure 7b) after 200 h of oxidation at 1000°C .

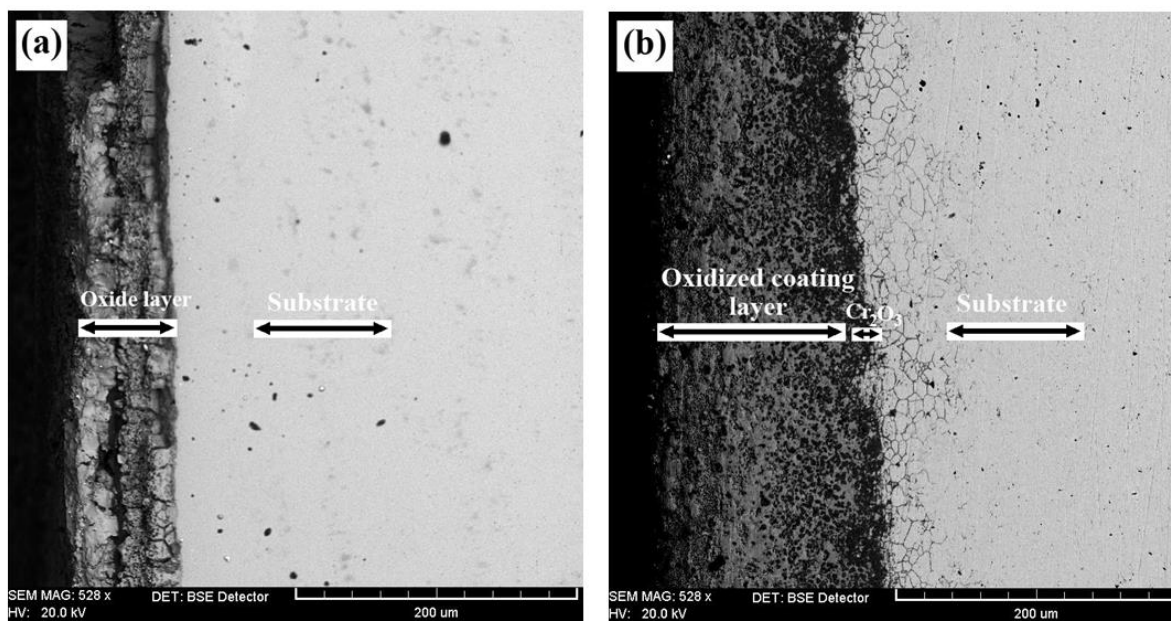


Fig. 7. SEM cross section image of the oxidized uncoated (a) Ti-coated (b) samples after 1000 h isothermal oxidation at 1000°C .

In the bare AISI 430 steel oxide scale has grown up to $\sim 70\ \mu\text{m}$. The spallation at the scale–metal interface (Fig. 7a) may have been created due to the creation of a silica network. SiO_2 is not miscible with Cr_2O_3 , and the poor adhesion between the oxides may cause the detachment of Cr_2O_3 from SiO_2 , which sticks to the steel during the progress of thermal stresses. The poor adhesion between Cr_2O_3 and SiO_2 is due to the difference between the thermal expansion coefficients (TEC). The TEC of silica ($0.55 \times 10^{-6}\ \text{}^\circ\text{C}^{-1}$) is lower than the TEC value of Cr_2O_3 ($9.6 \times 10^{-6}\ \text{}^\circ\text{C}^{-1}$) [4, 33]. Ferritic stainless steel has a TEC of $11 \times 10^{-6}\ \text{}^\circ\text{C}^{-1}$, which is relatively close to the TEC of chromia. Since SiO_2 is not entirely removed by the spalled scale, inadequate adhesion occurs between Cr_2O_3 and SiO_2 (silica is not

miscible with chromia). This poor adhesion, and the formation of a silica network at the alloy-scale interface, may be a reason for spallation of the scale [34].

For Ti-coated sample, coating layer, Cr_2O_3 scale layer and substrate can be distinguished (Fig. 7b). The top layer is the oxidized coating layer and beneath the coating layer, chromia layer has been developed. The thickness of the chromia scale layer is approximately $8\ \mu\text{m}$. Some cracks are observed between the oxidized coating layer and the chromia layer. The presence of chromium oxide at the interface with different ΔCTE value could be responsible for the formation of these cracks. SEM micrographs show the effectiveness of titanium coating in decreasing the outward diffusion of chromium (Fig. 7). The thickness of Cr_2O_3 oxide layer

is less than that of the uncoated sample because the coating layer restricted chromium diffusion.

3-3- Cyclic oxidation behavior

For studying the resistance of titanium coating during thermal stresses, the Ti-coated and

uncoated specimens were subjected to 50 cycles of oxidation. Each cycle included 1h heating at 1000 °C in the electrical furnace and 15 minutes cooling in air. Mass gain for the Ti-coated and uncoated specimens as a function of cyclic oxidation is demonstrated in Fig. 8.

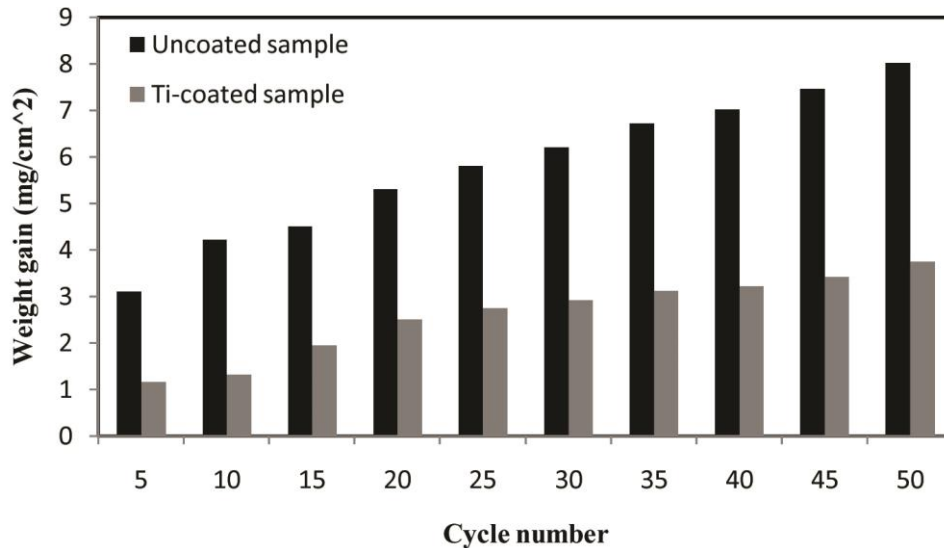


Fig. 8. Mass gain as a function of cycle number in cyclic oxidation for the uncoated and coated samples.

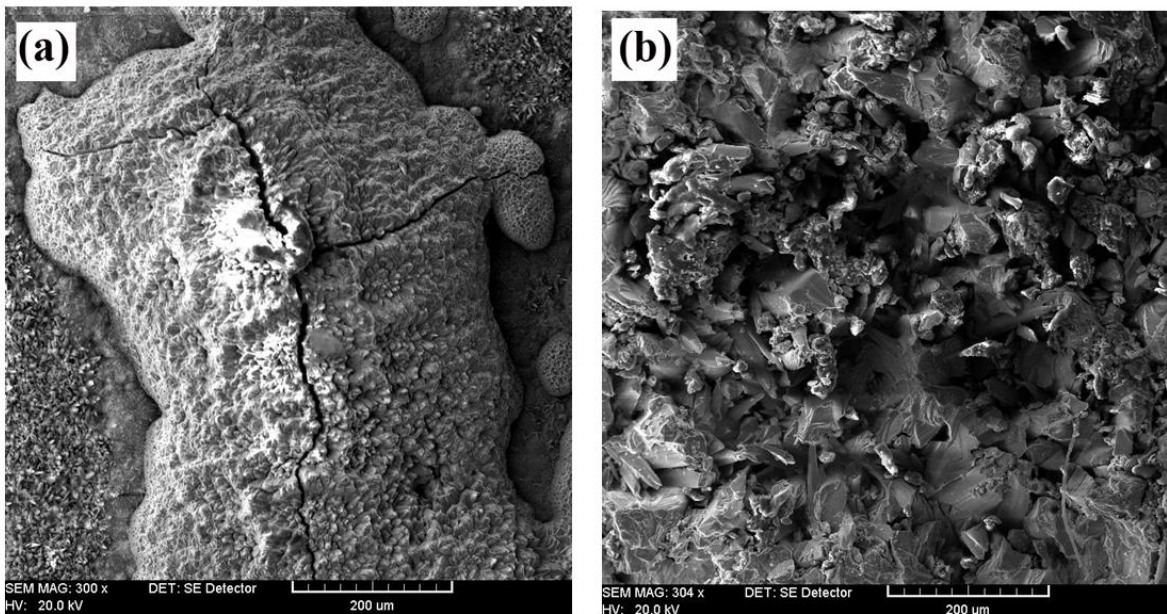


Fig. 9. SEM micrographs of the oxidized (a) uncoated and (b) Ti-coated samples after 50 cycles at 1000 °C.

As can be seen, the weight gain of the uncoated samples increases as the number of cycle increases. This occurs as a result of the growth of oxide scales and spallation. Spallation is the result of mismatching of thermal expansion

coefficient (TEC) of oxide scale and metallic substrate [32-34]. The mass gain for Ti-coated and uncoated specimens after 50 cycles was 3.74 mgcm⁻² and 8.01 mgcm⁻², respectively.

The surface of the uncoated specimen spalled from some part of the sample (Fig. 9a), while the surface of Ti-coated sample after 50 cycles showed good resistance against cracking and spallation (Fig. 9b). The created cracks in the surface of bare steel are probably related to the stresses originating from the differences in thermal expansion coefficient between the substrate and the formed oxides on the surface. Thermal expansion coefficient of iron oxides are larger than that of the stainless steel, resulting in tensile stresses in the oxide during cooling [35]. Spalled scale creates diffusion path for cations and anions and therefore through the simple migration of ions the oxide layer grows with a higher rate. Results of cyclic oxidation showed that titanium coating layer had good resistance against the thermal stresses which exhibit excellent thermal expansion coefficient (TEC) matching of titanium coating layer with substrate [34, 36-38]. Cracking and spallation in bare specimens may be because of silica network. Silica is not miscible with chromia [4]. Spalled scale creates diffusion paths for cations and anions and as a result of simple migration of ions, the oxide layer grows with a higher rate which results in higher values of weight gain.

4-Conclusions

1. AISI 430 stainless steel was coated with titanium through pack cementation method.
2. Ti coating consisted of two layers with the total thickness of 50 micrometers, which contained TiFe, TiFe₂ and Fe₂TiO₅ phases.
3. The formation of TiO₂, TiFe, TiFe₂, TiFe₂O₅ and Fe₂TiO₄ phases resulted in lower weight gain compared to the bare samples in isothermal oxidation.
4. In cyclic oxidation, Ti-coated samples demonstrated good resistance against the cracking and spallation and resulted in lower values of weight gain compared to the uncoated samples.

References

[1] F. Riffard, H. Buscail, H. Caudron, R. Cuffe, C. Issartel, S. Perrier, "The influence of implanted yttrium on the cyclic oxidation behaviour of 304 stainless steel", *Appl. Surf. Sci.*, Vol. 252, 2006, pp. 3697-3706.

[2] F.J. Pérez, M. Jcristóbal, M.P. Hierro, F. Pedraza, "The influence of implanted silicon on the cyclic oxidation behaviour of two different stainless steels", *Surf. Coat. Technol.* Vol. 442, 1999, pp. 120-121.

[3] D. Laverde, T. Gómez-Acebo T, F. Castro, "Continuous and cyclic oxidation of T91 ferritic steel under steam", *Corros. Sci.* Vol. 46, 2004, pp. 613-631.

[4] S. Fontana, R. Amendola, R. Chevalier, P. Piccardo, G. Cabocho, M. Vivani, R. Molins, M. Sennour, "Metallic interconnects for SOFC: Characterization of corrosion resistance and conductivity evaluation at operating temperature of differently coated alloys", *J. Power Sources.* Vol. 171, 2007, pp. 652-662.

[5] C. Houngrinou, S. Chevalier, J. Larpin, "Synthesis and characterisation of pack cemented aluminide coatings on metals", *Applied Surf. Sci.*, Vol. 236, 2004, pp. 256-269.

[6] M.R. Bateni, S. Mirdamadi, F. Ashrafizadeh, J.A. Szpunar, R.A.L. Drew., "Oxidation behaviour of titanium coated copper substrate", *Surf. Coat. Technol.*, Vol. 139, 2001, pp. 192-199.

[7] S.C. Kung, R.A. Rapp, "Fundamental kinetic study of aluminization of iron by pack cementation at 900 °C", *Surf. Coat. Technol.*, Vol. 32, 1987, pp. 41-56.

[8] A. Castle, D. Gabe, "Chromium diffusion coatings", *Int. Mater. Rev.*, Vol. 44, 1999, pp. 37-58.

[9] R.A. Rapp., "Kinetics microstructures and mechanism of internal oxidation, its effect and prevention in high temperature alloy oxidation", *Corrosion*, Vol. 21, 1965, pp. 382-401.

[10] R.M. Burns, W.W. Bradley, *Protective coatings for metals*. 3rd Edition, Reinhold Publishing Corporation, 1967.

[11] M. Zandrahimi, J. Vatandoost, H. Ebrahimifar, "Pack cementation coatings to improve high-temperature oxidation resistance of AISI 304 stainless steel", *J Mater. Eng. Perform.* Vol. 21, 2012, pp. 2074-2079.

[12] C.H. Koo, T.H. Yu, "Pack cementation coatings on Ti₃Al-Nb alloys to modify the high-temperature oxidation properties", *Surf. Coat. Technol.*, Vol. 126, 2000, pp.171-180.

[13] F.J. Pérez, M.P. Hierro, F. Pedraza, M.C. Carpintero, C. Gómez C, R. Tarín, "Effect of fluidized bed CVD aluminide coatings on the cyclic oxidation of austenitic AISI 304 stainless

- steel”, *Surf. Coat. Technol.*, Vol. 145, 2001, pp. 1–7.
- [14] T.L. Hu, H.L. Huang, D. Gan, T.Y. Lee, “The microstructure of aluminized type 310 stainless steel”, *Surf. Coat. Technol.*, Vol. 201, 2006, pp. 3502–3509.
- [15] F. Ustel, S. Zeytin, “Growth morphology and phase analysis of titanium-based coating produced by thermochemical method”, *Vacuum.*, Vol. 81, 2006, pp. 360–365.
- [16] H. Ebrahimifar, M. Zandrahimi, “Evaluation of the parabolic rate constant during different types of oxidation tests for spinel coated Fe-17%Cr alloy”, *Oxide Met.*, Vol. 75, 2010, pp.125-141.
- [17] H. Ebrahimifar, M. Zandrahimi, “Mn coating on AISI 430 ferritic stainless steel by pack cementation method for SOFC interconnect applications”, *Solid State Ionics*, Vol. 183, 2011, pp.71-79.
- [18] Z.G. Yang, “Recent advances in metallic interconnects for solid oxide fuel cells, *Int. Mater. Rev.* Vol. 53, 2008, pp.39-54.
- [19] J.L. Gonzalez-Carrasco, P. Perez, P. Adeva, J.Chao, Oxidation behaviour of an ODS NiAl-based intermetallic alloy”, *Intermetallics*. Vol. 7, 1999, pp. 69-78.
- [20] P.Y. Hou, K. Huang, W.T. Bakker, *Proceedings of the Sixth International Symposium on Solid Oxide Fuel Cells (SOFC VI)*, 1999, Honolulu, Hawaii, p.737.
- [21] A. Holta, P. Kofstada, “Electrical conductivity and defect structure of Cr₂O₃. II. Reduced temperatures (<~1000°C)”, *Solid State Ionics*. Vol. 69, 1994, pp.137-143.
- [22] W.J. Quadackers, J.P. Abellan, V. Shemet, L. Singheiser, Metallic interconnectors for solid oxide fuel cells, A review, *Mater. High Temp.*, Vol. 20, 2003, pp.115–127.
- [23] P. Jian, L. Jian, H. Bing, G. Xie, “Oxidation kinetics and phase evolution of a Fe–16Cr alloy in simulated SOFC cathode atmosphere, *J. Power Sources*, Vol. 158, 2006, pp.354–360.
- [24] A.C. Soares Sabionia, A.M. Huntz, E.C. da Luza, M. Mantel, C. Haut, “Comparative Study of High Temperature Oxidation Behaviour in AISI 304 and AISI 439 Stainless Steels”, *Mater. Res.*, Vol. 6, 2003, pp.179-185.
- [25] A. Balland, P. Gannon, M. Deibert, S. Chevalier, G. Caboche, S. Fontana, “Investigation of La₂O₃ and/or (Co,Mn)₃O₄ deposits on Crofer22APU for the SOFC interconnect application”, *Surface and Coatings Technology*, Vol. 203, 2009, pp.3291.
- [26] X. Deng, P. Wei, M.R. Bateni, A. Petric, “Cobalt plating of high temperature stainless steel interconnects”, *J. Power Sources*, Vol. 160, 2006, pp.1225-1229.
- [27] L. Cooper, S. Benhaddad, A. Wood, D.G. Ivey, “The effect of surface treatment on the oxidation of ferritic stainless steels used for solid oxide fuel cell interconnects”, *J. Power Sources*. Vol. 184, 2008, pp. 220-228.
- [28] M.G.C. Cox, B. Mckenney, V.D. Scott, “Chemical diffusion model for partitioning of transition elements in oxide scales on alloys”, *Phil Mag.* Vol. 26, 1972, pp. 839-851.
- [29] H. Kurokawa, K. Kawamura, T. Maruyama, “Oxidation behavior of Fe–16Cr alloy interconnect for SOFC under hydrogen potential gradient”, *Solid State Ionics*. Vol. 168, 2004, pp.13-21.
- [30] T. Horita, Y. Xiong, K. Yamaji, N. Sakai, H. Yokokawa, “Evaluation of Fe-Cr alloys as interconnects for reduced operation temperature SOFCs”, *J. Electrochem. Soc.*, Vol. 150, 2003, pp.243-248.
- [31] J.H. Westbrook, R.L. Fleischer, “Intermetallic compounds: principles and practice”, Vol. 3, *Progress*. 2002: Wiley
- [32] H. Ebrahimifar, M. Zandrahimi, “Oxidation and electrical behavior of AISI 430 coated with cobalt spinels for SOFC interconnect applications”, *Surf. Coat. Technol.*, Vol. 206, 2011, pp. 75-81.
- [33] N. Shaigan, D.G. Ivey, W. Chen, “A review of recent progress in coatings, surface modifications and alloy developments for solid oxide fuel cell ferritic stainless steel interconnects” *J. power sources*, Vol. 195, 2010, pp.1529-1542.
- [34] N. Shaigan, D.G. Ivey, W. Chen, “Oxidation and electrical behavior of nickel/lanthanum chromite coated stainless steel interconnects”, *J. power sources*, Vol. 183, 2008, pp. 651-659.
- [35] J. Zurek, E. Wessel, L. Niewolak, F. Schmitz, T.-U. Kern, L. Singheiser, W.J. Quadackers, “Anomalous temperature dependence of oxidation kinetics during steam oxidation of ferritic steels in the temperature range 550–650 °C”, *Corros. Sci.* Vol. 46, 2004, 2301-2317.

- [36] E. N'Dah, S. Tsipas, M.P. Hierro, F.J. Pérez, "Study of the cyclic oxidation resistance of Al coated ferritic steels with 9 and 12%Cr", *Corros. Sci.*, Vol. 49, 2007, pp.3850-3865.
- [37] V.A. Ravi, *ASM Handbook. Packcementation Coating*. Vol. 13. pp.763-771.
- [38] C.H. Koo and T.H. Yu, "Pack Cementation Coatings on Ti₃Al-Nb Alloys to Modify the High-Temperature Oxidation Properties", *Surf. Coat. Technol.*, Vol. 126, 2000, pp. 171–180.